

Diffusion-VLA: Scaling Robot Foundation Models via Unified Diffusion and Autoregression

Junjie Wen^{1,2,*}, Minjie Zhu^{1,2,*}, Yichen Zhu^{2,†,*}, Zhibin Tang², Jinming Li^{2,3}, Zhongyi Zhou^{1,2},
Chengmeng Li^{2,3}, Xiaoyu Liu^{2,3}, Yaxin Peng³, Chaomin Shen¹, Feifei Feng²

¹East China Normal University, ²Midea Group, ³Shanghai University

<https://diffusion-vla.github.io>

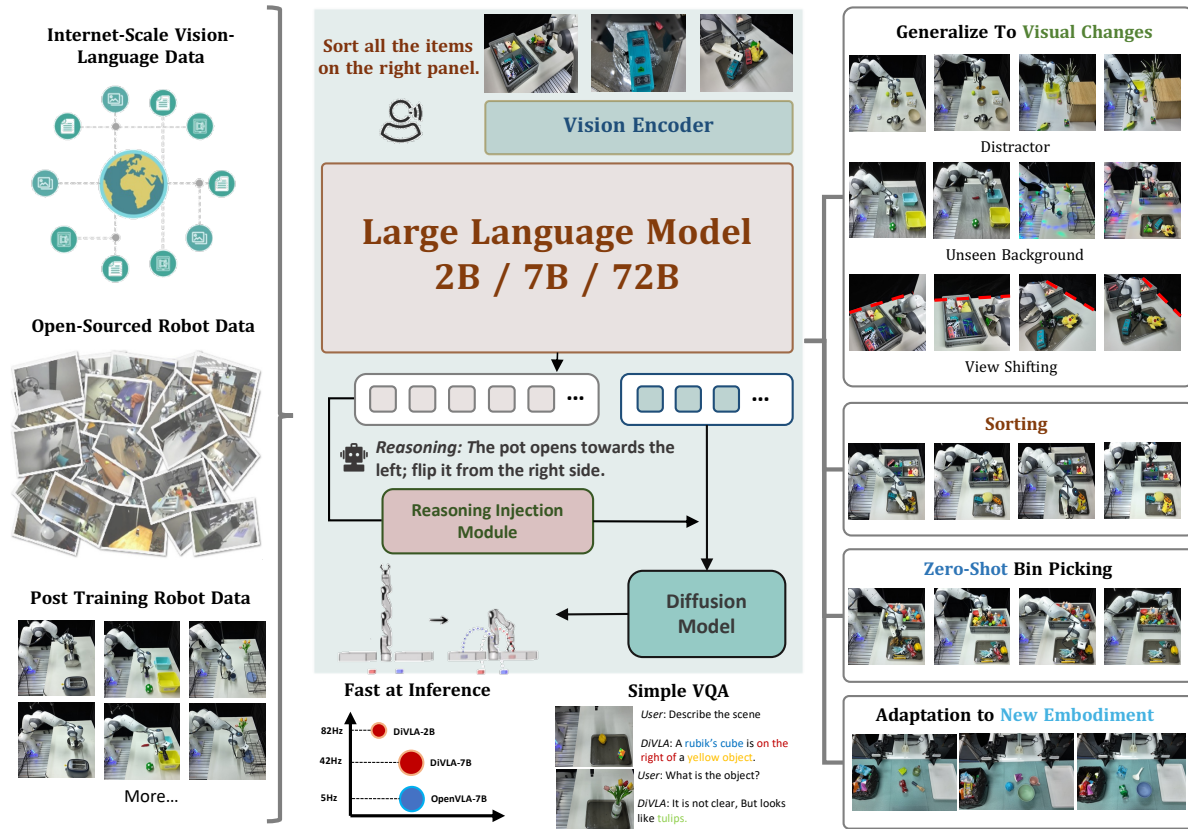


Figure 1. Our proposed DiffusionVLA model unifies autoregressive and diffusion modeling to enable self-reasoning and robot policy learning. This approach generalizes effectively to visual changes, supports zero-shot bin picking, adapts to new robot morphologies, performs visual question-answering, and generates actions with high speed.

Abstract

In this paper, we present DiVLA, a novel framework that seamlessly combines the autoregression model with the diffusion model for learning visuomotor policy. Central to our approach is a next-token prediction objective, enabling the model to reason effectively over the user’s query in the context of current observations. Subsequently, a diffusion

model is attached to generate robust action outputs. To enhance policy learning through self-reasoning, we introduce a novel reasoning injection module that integrates reasoning phrases directly into the policy learning process. The whole framework is simple and flexible, making it easy to deploy and upgrade.

We conduct extensive experiments using multiple real robots to validate the effectiveness of DiVLA. Our tests include a challenging factory sorting task, where DiVLA suc-

*: Co-first author. †: Corresponding Author.

successfully categorizes objects, **including those not seen during training**. We observe that the reasoning module enhances interpretability, allowing observers to understand the model’s thought process and identify potential causes of policy failures. Additionally, we test DiVLA on a zero-shot bin-picking task, achieving **63.7% accuracy on 102 previously unseen objects**. Our method demonstrates robustness to visual changes, such as distractors and new backgrounds, and easily adapts to new embodiments. Furthermore, DiVLA can follow novel instructions and retain conversational ability. Notably, DiVLA is data-efficient and fast at inference; our smallest DiVLA-2B runs **82Hz on a single A6000 GPU** and can train from scratch on less than 50 demonstrations for a complex task. Finally, we scale the model from 2B to 72B parameters, showcasing improved generalization capabilities with increased model size.

1. Introduction

Autoregressive models are predominant in Large Language Models, operating by sequentially predicting discrete tokens, where each token generation depends on the preceding ones. This approach has also influenced robotics, leading to the development of Vision-Language-Action (VLA) models, which frame action prediction as a next-token prediction task. While these models, i.e., RT-2 [9] and OpenVLA [26], have achieved notable success, they face intrinsic limitations. First, discretizing continuous action data into fixed-size tokens disrupts the coherence and precision of actions. Second, NTP is inherently inefficient for action generation, especially in real-time robotic applications where performance is critical.

Meanwhile, building on the success of diffusion models in content generation [15, 16, 36, 38, 43], diffusion-based models for learning visuomotor policies [10] have gained significant popularity over the past two years. Numerous methods have demonstrated strong performance in manipulation tasks by modeling action sequence generation as a noise-denoising process. This approach better captures the multimodal nature of robotic actions and enables faster sequence generation compared to NTP-based VLA models. However, despite the advantages of diffusion models for policy learning, they lack the reasoning capabilities crucial for VLA models to solve complex tasks effectively, a component that evidently improves LLMs.

This motivates us to raise the question: *can we bring together the advantages of both parties, specifically the reasoning power of autoregressive models and the robustness of high-frequency action generation offered by diffusion models?*

In this work, we propose a unified model, named *DiffusionVLA (DiVLA in short)*, that integrates autoregression with a diffusion model. The autoregressive compo-

nent provides reasoning over the query, while the diffusion model controls the robot. Specifically, DiVLA builds upon a pre-trained Vision-Language Model (VLM), retaining its autoregressive capabilities for text-based reasoning. We extend this foundation by integrating a diffusion model that facilitates learning robotic actions through a noise-denoising process. This setup empowers DiVLA to achieve both language-driven reasoning and robust action generation in robotic contexts. However, simply combining these elements does not fully exploit the reasoning potential, as there is often an implicit gap between logical reasoning and actionable robot policies. To bridge this gap, we propose a reasoning injection module, which reuses reasoning outputs and embeds them directly into the policy head, thus enriching the policy learning process with explicit reasoning signals. This innovation allows us to directly incorporate reasoning into action generation, enhancing the model’s dexterity, robustness, and generalization across various scenarios. Our experiments confirm that DiVLA delivers the following advantages:

- **Fast Inference Speed:** DiVLA-2B achieves an inference rate of 82Hz, and DiVLA-7B operates at 42Hz on a single A6000 GPU, ensuring real-time responsiveness in high-demand environments.
- **Enhanced Visual Generalization:** DiVLA is unaffected by visual distractions or novel backgrounds, demonstrating robustness in visually dynamic settings.
- **Generalizable Reasoning Capability:** DiVLA can recognize and categorize previously unseen objects accurately, showcasing its ability to generalize reasoning across novel inputs.
- **Adaptability to Novel Instructions and Conversational Capability:** Our approach can interpret and execute complex, novel instructions while maintaining conversational fluency, offering a versatile response range in interactive scenarios.
- **Generalization to Other Embodiment:** DiVLA readily fine-tunes for deployment on real bimanual robots, achieving high performance with minimal adjustment, proving its adaptability across diverse robotic embodiments.
- **Scalability:** We provide a scalable family of models — DiVLA-2B, 7B, and 72B — demonstrating that generalization and performance improve with model size, adhering to established scaling laws.

We believe that DiVLA offers a novel perspective on the learning and generalizing robot policy.

2. Related Works

Autoregression models. Predicting the next token has been regarded as a key approach toward general artificial intelligence due to its success in training language models [1, 4, 47–49]. RT-2 [9] pioneered the application of next-

token prediction in robot learning which predicts actions by converting continuous actions into discrete tokens for learning robotic motion. Building on this, OpenVLA [26] introduced an open-source, improved, and smaller version of RT-2 [9] with a similar approach, while ECoT [64] developed a chain-of-thought method. However, research has shown that next-token prediction may not be the optimal approach for robot models, especially when adapting to various embodiments. In this work, we leverage the strength of next-token prediction specifically for reasoning tasks.

Diffusion models. Diffusion models have become dominant in the field of visual generation. The Diffusion Policy [10] extends the application of diffusion models to robot learning, demonstrating their effectiveness in handling multimodal action distributions. Subsequent work has advanced the Diffusion Policy [5, 6, 11, 30, 39, 42, 50, 51, 55, 71] by applying it to 3D settings [24, 62, 66, 68], scaling it up [74], increasing its efficiency [21, 56], and introducing architectural innovations. For instance, TinyVLA [57] integrates diffusion models with lightweight vision-language models, while pi_0 [7] leverages flow matching rather than diffusion for action generation. Our approach introduces reasoning—a crucial element in language models—into the diffusion-based vision-language-action (VLA) model.

Robot foundation models. Existing works [3, 8, 9, 12, 14, 20, 22, 75] leverage RL [19, 32, 41, 45, 63, 65, 67] and LLM [2, 18, 23, 29, 40, 58, 73] to decouple the multimodal understanding and embodied control. Another line of research leverages pre-trained Vision-Language Models (VLMs) and fine-tunes them directly on robotic data [9, 26, 57, 64]. Our work follows this approach, unifying autoregressive and diffusion models for both reasoning and manipulation tasks.

Unified auto-regressive model and image generation. Recent work has focused on unifying multimodal understanding with image generation. These efforts include using auto-regressive methods to generate images [28, 33, 46, 52, 54], diffusion models to produce text, or combining both approaches into unified models [13, 31, 59, 70], such as Show-O [61], Transfusion [72], and Vila-U [60]. Unlike these methods, our framework explores unifying next-token prediction with diffusion models, which enhances the robot model’s reasoning abilities. This reasoning capability, in turn, improves the model’s generalization to various tasks and environments.

3. Methodology

Our ultimate goal is to create a unified framework that combines autoregressive models, which excel at predicting language sequences for reasoning, with diffusion models, which are highly effective at generating robotic actions. Developing such an integrated model presents substantial challenges, with key issues centered on: (i) designing an

architecture that seamlessly and efficiently integrates both autoregressive and diffusion mechanisms; and (ii) leveraging self-generated reasoning to enhance action generation without adding inference computation overhead. In this section, we introduce the overall framework of our method in Section 3.1 and explore the design choices that inform our model architecture in Section 3.2.

3.1. Architecture

Given any sequence of interleaved images, text, and video, we first encode the images into dense visual features using SigLIP [69]. These encodings are then transformed into a fixed number of N visual embeddings through a Transformer. It’s worth noting that typical visual inputs in robot learning often include multiple camera views. To manage this, we applied the shared SigLIP visual backbone to each view and subsequently concatenated the resulting visual tokens.

For vision-language processing, we leveraged Qwen2-VL [53], a state-of-the-art vision-language model available in three sizes: 2B, 7B, and 72B parameters. We initialized the VLM backbone with the publicly released checkpoint. It is also possible to use any other pre-trained VLM as backbone, since we decouple the vision-language understanding with action generation, making the overall architecture flexible to fit for advanced new models.

Action decoder. We employ a latent diffusion model to decode visual and instruction embeddings into actions. Specifically, we generate a set of tokens using an LLM and feed these tokens into the diffusion model as conditioning inputs for action decoding. Our architecture follows the design of the standard Diffusion Policy [10], with randomly initialized model weights. This component also incorporates reasoning from the LLM, which we describe in detail below. An MLP layer is attached to the last layer at the bottom of the action decoder to predict the robot’s joint space. If multiple embodiments are evolved, instead of making a copy of a separate action decoder [34], we simply initialized a new MLP layer for training and evaluation. This step ensures that the knowledge from the pre-trained data is preserved and thus can quickly adapt to a new embodiment.

Reasoning injection module. The core of our approach lies in introducing explicit reasoning into Vision-Language-Action (VLA) models. Unlike most autoregressive VLAs, which require a recursive setup — converting reasoning outputs into inputs for subsequent model runs — our method proposes a more efficient and streamlined integration of reasoning. By embedding reasoning directly within the policy model, we avoid the computational and operational complexities of iterative input-output cycles,

enabling faster and more seamless reasoning incorporation.

Our reasoning injection module operates by taking the final embedding from the tokenized output of the reasoning component and directly injecting it into the policy model through Feature-wise Linear Modulation (FiLM) [37]. This injection technique, inspired by methods in RT-1 [8] and YAY [44], enables us to modulate the policy network’s layers based on the reasoning signal. We refer to this process as “injection” because, in our design, the policy network focuses primarily on action-specific tokens, while the reasoning module functions as an auxiliary enhancement, providing contextual depth without dominating the primary decision-making flow. This approach ensures that reasoning is not only present but actively utilized during policy model training.

3.2. Model Design Choices

We illustrate the training strategy and other techniques that we used to improve the efficiency and effectiveness of our method. We also discuss the selection of pretraining data.

View-adaptive tokenization. As experiments in robot policy learning commonly use multiple camera views. As the number of views increases, the count of visual tokens also rises, leading to significant computational overhead due to the complexity of self-attention. To address this, we propose a view-adaptive tokenization method that reduces the number of visual tokens, optimizing computational efficiency.

Our approach is straightforward yet effective: we significantly reduce the number of tokens for wrist camera views to just 16, which is over 20 times fewer than those for extrinsic views. This reduction is motivated by the distinct role of the wrist camera, which primarily assists in precise localization for grasping tasks. High-resolution processing of wrist views, while detailed, is often inefficient and consumes resources that could be better allocated to processing more critical visual signals from external perspectives.

This optimization is particularly beneficial in dual-arm robotic systems, where two wrist cameras are active simultaneously. By reducing the computational load associated with wrist views, we free up resources to handle other essential tasks, enabling smoother, more efficient operation and potentially enhancing the overall responsiveness and precision of the robotic system.

Training objectives. Given a batch of input sequences, the overall training loss is formulated as a combination of the diffusion loss and the next-token prediction loss: $L = L_{diff} + \alpha L_{ntp}$, where α is the hyper-parameters weighting the loss term L_{ntp} . In our observations, the magnitude of L_{ntp} consistently remains about ten times smaller than that of L_{diff} . To balance the contribution

of each component to the overall loss, we typically set $\alpha = 1$ in all experiments. This adjustment ensures that both terms are comparably weighted in the training process, allowing the model to learn effectively from both action and next-token prediction tasks.

Pretraining Data. We consider OXE [35] and Droid [25] dataset for pretraining. We use Droid data to pre-train DiVLA-2B and DiVLA-7B. For DiVLA-72B, we use OXE and Droid together for pre-train. The original Droid data contains only robotic actions, paired partially with observations and language instructions. These data contain only robotic actions, paired partially with observations and language instructions. To enhance our model’s ability to generalize with language, we leverage GPT-4o to automatically transform these data into a form that includes reasoning. Consequently, the network architecture remains consistent across both the pre-training and fine-tuning stages.

4. Experiments

In this section, we examine the effectiveness of DiVLA for embodied control. In Section 4.2, we compare DiVLA against other state-of-the-art models within a standard multi-task setting, assessing its performance in both in-distribution and out-of-distribution scenarios. In Section 4.3, we evaluate DiVLA in the challenging sorting task, showcasing its remarkable performance and illustrating how reasoning enables the model to analyze robot actions and sort items accurately. In Section 4.4, we showcase DiVLA’s impressive generalization abilities in a zero-shot bin-picking task involving over 102 unseen objects. In Section 4.5, we illustrate DiVLA’s adaptability to new embodiments, successfully completing complex tasks that require bimanual coordination. We provide experimental setup and implementation details in the Appendix.

4.1. Experimental Setup.

Implementation details and pretraining data. The model is pre-trained on the Droid [25] dataset. We then finetune our model on evaluation tasks, similar to the setting as π_0 [7]. We use LoRA [17] to fine-tune the VLM models. We use $2e-5$ as a fixed learning rate to pretrain the model.

Data for finetuning. We explore four experimental settings: sorting, bin picking, multi-task learning, and table bussing. The first three settings are conducted with the Franka robot, while the table bussing task utilizes the bimanual AgileX robot. Our dataset includes 500 trajectories for the sorting task and 580 trajectories for multi-task learning. The bin picking task is designed as a zero-shot task, so no training data was collected for it. For the table bussing task, we gathered 400 trajectories,

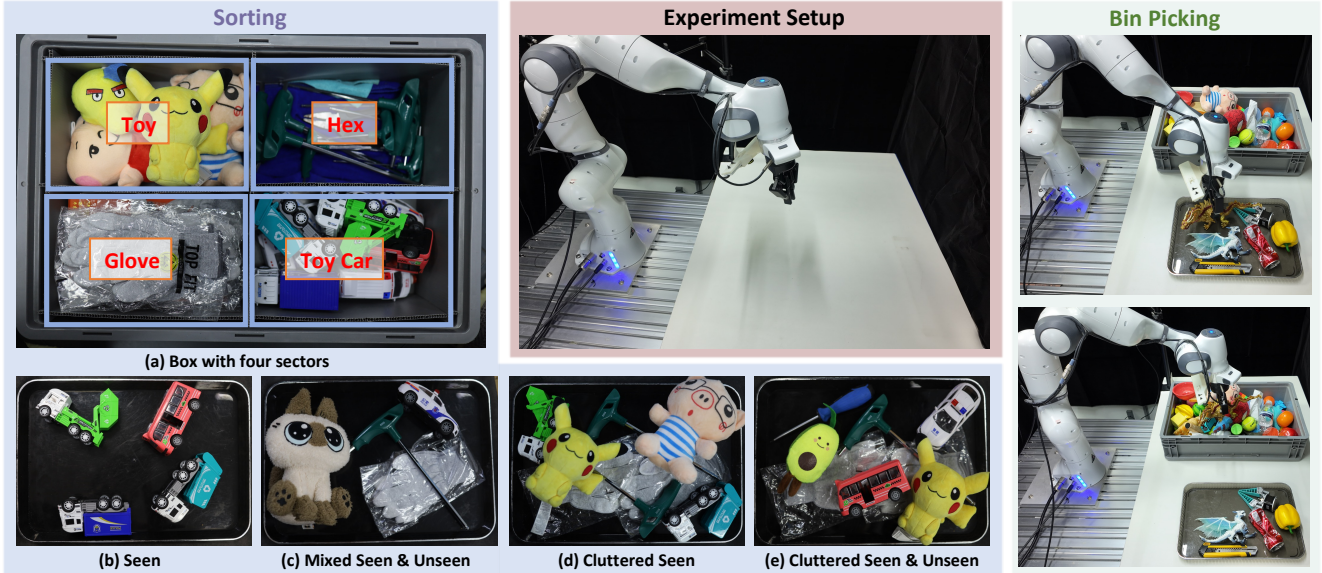


Figure 2. **Environmental setup for the Franka Robot and experimental configuration for sorting/bin-picking.** **Left:** For factor sorting tasks, (a) The target sorting box is divided into four distinct sectors, each designated for one of the following categories: stuffed toys, hex keys, knit gloves, and toy cars, (c) The seen objects in the train data, (d) mixing the seen and unseen object for evaluation, (e) cluttered scene for seen objects, (f) cluttered scene for mixing seen and unseen objects. **Middle:** We use a Franka robot arm equipped with two external Zed cameras and a Realsense 435i wrist camera. **Right:** The setup for zero-shot bin picking.

where objects are randomly placed on the table, often overlapping with each other. During the fine-tuning stage, all data corresponding to the same embodiment are trained together. For instance, the sorting and multi-task data are combined for training purposes.

4.2. Real-World Multi-Task Learning

We begin with a standard setting in which the model is trained on multiple tasks and completes each task based on different user queries. We designed five tasks: object selection, flip the vertically placed pot, placing a cube into a designated box, placing a cup onto a plate, and placing a cube inside a box. Detailed descriptions of these tasks are provided in the Appendix. The experimental results can be found in Table 1.

We compare our method to the Diffusion Policy [10], TinyVLA [57], Octo [34], and OpenVLA [26]. Notice that both Octo and OpenVLA is pre-trained on OXE [35], which is 25 times larger than our pre-trained datasets.

Generalization to visual changes. We further evaluate our method in a multi-task setting with visual changes to assess its robustness and adaptability in diverse, dynamic environments. Specifically, we introduce three challenging scenarios designed to test the model’s ability to handle visual variability: 1) adding additional distractors in the surroundings to increase visual clutter and complexity, 2) altering the background to test resilience against shifts in

scene context, and 3) implementing colorful lighting effects to introduce varied illumination and color hues. These scenarios are shown in Figure 5 to illustrate the impact of each change on the visual environment. The experimental results are demonstrated in Table 1.

Our evaluation of these scenarios reveals that while all methods experience a decline in performance due to these visual changes, our method consistently maintains the highest average success rate across five different tasks. This outcome highlights the model’s inherent robustness and adaptability, despite the absence of any specific data augmentation techniques during training.

4.3. End-to-End Sorting on Real Robot

We evaluate the capability of DiVLA in an industrial setting, where a robot is tasked with sorting items into designated sectors within a large box based on object category. Specifically, we categorize items into four classes: (1) toy cars, (2) knit gloves, (3) stuffed toys, and (4) hex keys. The language instruction provided is “Sort all items into corresponding areas”. A total of 500 trajectories are collected as training data. The task is considered successful only if the robot successfully grasps the object and places it in the correct sector. The experimental setup is illustrated in Figure 2.

This task poses several challenges, requiring both precise object grasping and accurate category identification. We assess our method under two difficulty settings: easy and hard. In easy mode, fewer than 5 items are placed on

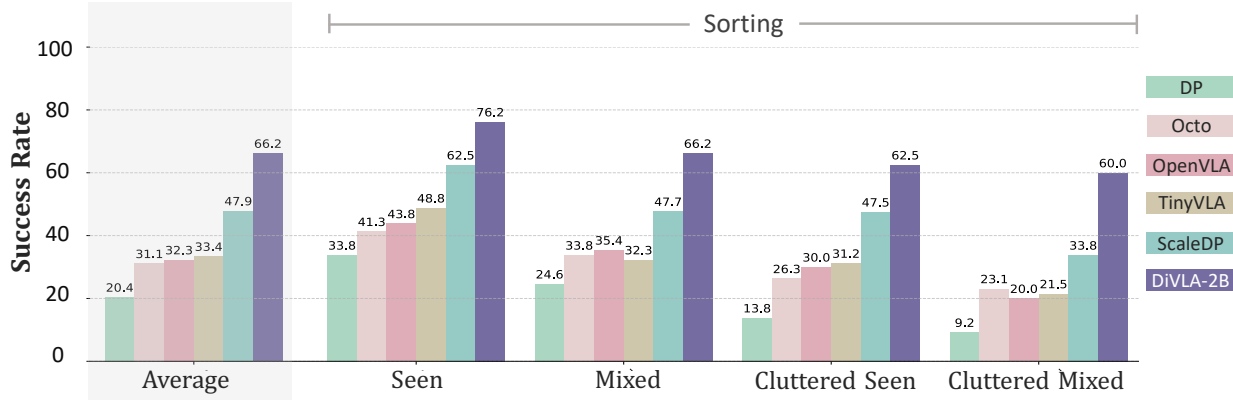


Figure 3. **Experimental results for sorting.** We compared our DiVLA with Diffusion Policy, Octo, TinyVLA, and OpenVLA. DiVLA achieves the highest average success rate, outperforming the runner-up OpenVLA by 20.9%.

Table 1. **Experimental results for multi-task learning on real robot.** We report the count of pre-trained trajectories. We also report the average success rate for evaluation on both in-distribution and out-of-distribution. Task 1: Select the appropriate object based on the user’s intent. Task 2: Flip the vertically placed pot. Task 3: Pick up the cube and place it into the [yellow/blue] box. Task 4: Place the cup onto the plate. Task 5: Place the cube into the box.

Model \ Tasks	Pre-trained Trajectory	In-Distribution					Avg.	Visual Generalization					Avg.
		Task 1	Task 2	Task 3	Task 4	Task 5		Task 1	Task 2	Task 3	Task 4	Task 5	
Diffusion Policy [10]	-	66.7	36.4	0	36.4	0	27.9	11.1	11.1	0	22.2	0	8.9
ScalingDP-1B [74]	-	66.7	36.4	27.3	37.0	18.2	35.2	33.3	33.3	0	22.2	22.2	22.2
TinyVLA [57]	-	72.7	45.5	36.4	45.5	27.3	45.5	44.4	44.4	11.1	22.2	22.2	28.9
Octo [34]	970K	57.6	27.3	9.1	0	27.3	24.3	44.4	11.1	11.1	0	22.2	17.8
OpenVLA-7B [26]	970K	69.7	18.2	18.2	36.4	54.5	39.4	55.6	11.1	0	33.3	33.3	26.7
DiVLA-2B	39K	100	100	63.6	63.6	90.9	83.6	44.4	66.7	44.4	66.7	66.7	57.8
DiVLA-7B	39K	100	100	72.7	81.8	100	90.9	66.7	88.9	55.6	77.8	66.7	71.0

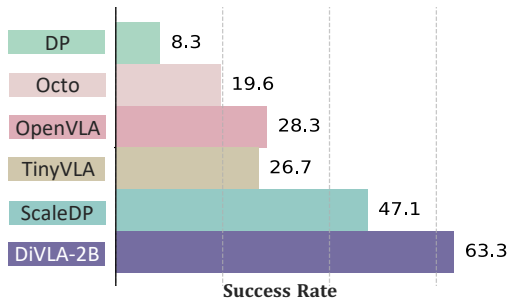


Figure 4. **Zero-shot bin picking on 102 unseen objects.** Our method outperforms the state-of-the-art robot foundation models by a large margin.

the table, whereas in hard mode, 6 to 11 items are randomly arranged. Furthermore, both seen and unseen objects are mixed in these scenarios. In the cluttered scene, items may overlap or be randomly distributed across the table, increasing the complexity of the sorting task.

The experimental results are illustrated in Figure 3.



Figure 5. **Examples of visual variations,** including randomly placed distractors, distracting lighting, and a colorful background on the right. DiVLA is robust to visual changes in different scenarios.

DiVLA demonstrates robust performance with an average success rate of 66.2% across all experimental settings. While other methods show significant performance degradation as scene complexity increases (i.e., higher object count and clutter level), particularly evident in DP’s sharp decline to 9.2% success rate in highly cluttered mixed scenarios, DiVLA maintains a substantial 60% success rate. This sustained performance underscores our approach’s

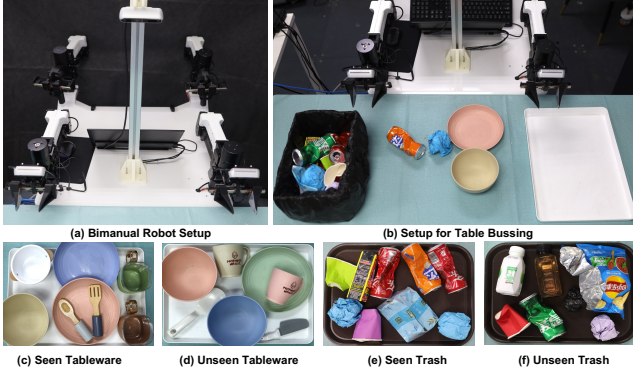


Figure 9. (a) Environmental setup for the bimanual robot, featuring three camera views; (b) Table bussing setup, with a trash bin positioned on the right side and a panel on the left. The task requires placing all tableware on the panel and all trash in the trash bin; (c-f) All tableware and trash items used in the bussing table task evaluation.

potential for applications in dynamic, unstructured environments where robots encounter unfamiliar objects and must perform tasks with minimal human intervention.

4.5. Adapt to Real-World Bimanual Robot

In this section, we examine DiVLA’s adaptability to a dual-arm robot. Inspired by π_0 [7], we designed a table bussing task that involves clearing table with various objects. This task was adapted for a bimanual robot setup: all tableware should be placed on a panel to the left, while trash items are dropped into a bin on the right. Similar to our factory sorting task, we evaluated the model’s performance using both seen objects and a combination of seen and unseen objects. The environment setup, along with all objects used for training and evaluation, is shown in Figure 9. Our evaluation consisted of twelve trials, with three to five objects randomly placed on the table. The success rate is computed by how many objects are correctly placed.

Our experimental results show that our model successfully completes tasks in most cases when the object has appeared in the training data, achieving an average success rate of 72.9% on seen objects. In contrast, the Diffusion Policy and OpenVLA achieve 45.8% and 0% success rates. For tasks involving both seen and unseen objects, DiVLA achieves up to a 70.8% success rate, a slight decrease in success rate compared to the seen one, showing remarkable generalization to objects with different colors and shapes. Finally, DiVLA demonstrates the ability to recognize unseen objects, particularly by responding sensitively to object color. For example, it categorizes a Sprite can as a “green can” and correctly places it in the trash bin. This observation further supports the idea that reasoning contributes to generalization.

Table 3. **Experimental results for Table Bussing on real bimanual robot.** Our method significantly outperforms both Diffusion Policy and OpenVLA by a large margin.

Scenarios	Diffusion Policy	OpenVLA	DiVLA-2B
Seen	45.8	0	72.9
Mixed	31.2	0	70.8

4.6. Following Novel Instruction

The previous section primarily evaluated the model’s performance on in-distribution task commands. In this section, we assess the model’s ability to follow novel instructions, specifically focusing on its generalization to previously unseen commands. We introduce new instructions that prompt the model to

We tested the model on four objects: 1) a watermelon, 2) a lemonade, 3) a blue paper trash, and 4) a red pepper. This is an extremely challenging task, as these novel instructions are absent from both the Droid dataset and our collected data. We evaluated four new instructions, with results summarized in Table 2.

Our findings indicate that both OpenVLA and DiVLA-2B can recognize these unseen objects and perform basic pick-and-place tasks. However, when it comes to complex sequential tasks, OpenVLA fails to interpret the instructions accurately; instead, it randomly selects items. In contrast, our method correctly follows the instructions, picking up objects in the specified sequence. We hypothesize that by learning to decompose long tasks into subtasks, our method acquires a generalized ability to understand complex, multi-step instructions. While OpenVLA can execute simpler commands like ‘Pick up the watermelon,’ it struggles with more advanced instructions requiring item selection in a specific order. Additionally, we observe a decrease in grasping precision when the model processes novel instructions, indicating that the novelty of instructions introduces further complexity to task execution.

5. Conclusion

In this work, we present DiVLA, a state-of-the-art vision-language-action model that delivers strong performance in both simulations and real-world scenarios, including single-arm and dual-arm robots. The core of our method lies in combining the next-token prediction objectives and diffusion models: the former for task reasoning and the latter for action prediction. We introduce a reasoning reuse module to enhance action generation and implement view-adaptive tokenization to reduce computational costs. Through extensive evaluations in both simulations and across multiple real-world embodiments, we demonstrate that DiVLA outperforms several SOTA robot models. Additionally, we show that DiVLA has robust generalization capabilities,

adapting effectively to new instructions, tasks, and environments. Our research offers a novel perspective on designing VLA models, encouraging a rethinking of how reasoning can be reused to facilitate end-to-end policy learning.

References

- [1] Josh Achiam, Steven Adler, Sandhini Agarwal, Lama Ahmad, Ilge Akkaya, Florencia Leoni Aleman, Diogo Almeida, Janko Altenschmidt, Sam Altman, Shyamal Anadkat, et al. Gpt-4 technical report. *arXiv preprint arXiv:2303.08774*, 2023. 2
- [2] Michael Ahn, Anthony Brohan, Noah Brown, Yevgen Chebotar, Omar Cortes, Byron David, Chelsea Finn, Chuyuan Fu, Keerthana Gopalakrishnan, Karol Hausman, et al. Do as i can, not as i say: Grounding language in robotic affordances. *arXiv preprint arXiv:2204.01691*, 2022. 3
- [3] Suneel Belkhale, Tianli Ding, Ted Xiao, Pierre Sermanet, Quon Vuong, Jonathan Tompson, Yevgen Chebotar, Debiddatta Dwibedi, and Dorsa Sadigh. Rt-h: Action hierarchies using language. *arXiv preprint arXiv:2403.01823*, 2024. 3
- [4] Xiao Bi, Deli Chen, Guanting Chen, Shanhuang Chen, Damai Dai, Chengqi Deng, Honghui Ding, Kai Dong, Qiusi Du, Zhe Fu, et al. Deepseek llm: Scaling open-source language models with longtermism. *arXiv preprint arXiv:2401.02954*, 2024. 2
- [5] Kevin Black, Michael Janner, Yilun Du, Ilya Kostrikov, and Sergey Levine. Training diffusion models with reinforcement learning. *arXiv preprint arXiv:2305.13301*, 2023. 3
- [6] Kevin Black, Mitsuhiko Nakamoto, Pranav Atreya, Homer Walke, Chelsea Finn, Aviral Kumar, and Sergey Levine. Zero-shot robotic manipulation with pretrained image-editing diffusion models. *arXiv preprint arXiv:2310.10639*, 2023. 3
- [7] Kevin Black, Noah Brown, Danny Driess, Adnan Esmail, Michael Equi, Chelsea Finn, Niccolo Fusai, Lachy Groom, Karol Hausman, Brian Ichter, Szymon Jakubczak, Tim Jones, Liyiming Ke, Sergey Levine, Adrian Li-Bell, Mohith Mothukuri, Suraj Nair, Karl Pertsch, Lucy Xiaoyang Shi, James Tanner, Quan Vuong, Anna Walling, Haohuan Wang, and Ury Zhilinsky. π_0 : A vision-language-action flow model for general robot control, 2024. 3, 4, 8
- [8] Anthony Brohan, Noah Brown, Justice Carbajal, Yevgen Chebotar, Joseph Dabis, Chelsea Finn, Keerthana Gopalakrishnan, Karol Hausman, Alex Herzog, Jasmine Hsu, et al. Rt-1: Robotics transformer for real-world control at scale. *arXiv preprint arXiv:2212.06817*, 2022. 3, 4
- [9] Anthony Brohan, Noah Brown, Justice Carbajal, Yevgen Chebotar, Xi Chen, Krzysztof Choromanski, Tianli Ding, Danny Driess, Avinava Dubey, Chelsea Finn, et al. Rt-2: Vision-language-action models transfer web knowledge to robotic control. *arXiv preprint arXiv:2307.15818*, 2023. 2, 3, 4
- [10] Cheng Chi, Siyuan Feng, Yilun Du, Zhenjia Xu, Eric Cousineau, Benjamin Burchfiel, and Shuran Song. Diffusion policy: Visuomotor policy learning via action diffusion. *arXiv preprint arXiv:2303.04137*, 2023. 2, 3, 5, 6
- [11] Sudeep Dasari, Oier Mees, Sebastian Zhao, Mohan Kumar Srirama, and Sergey Levine. The ingredients for robotic diffusion transformers. *arXiv preprint arXiv:2410.10088*, 2024. 3
- [12] Zipeng Fu, Tony Z Zhao, and Chelsea Finn. Mobile aloha: Learning bimanual mobile manipulation with low-cost whole-body teleoperation. *arXiv preprint arXiv:2401.02117*, 2024. 3
- [13] Yuying Ge, Sijie Zhao, Jinguo Zhu, Yixiao Ge, Kun Yi, Lin Song, Chen Li, Xiaohan Ding, and Ying Shan. Seed-x: Multimodal models with unified multi-granularity comprehension and generation. *arXiv preprint arXiv:2404.14396*, 2024. 3
- [14] Jiayuan Gu, Sean Kirmani, Paul Wohlhart, Yao Lu, Montserrat Gonzalez Arenas, Kanishka Rao, Wenhao Yu, Chuyuan Fu, Keerthana Gopalakrishnan, Zhuo Xu, et al. Rt-trajectory: Robotic task generalization via hindsight trajectory sketches. *arXiv preprint arXiv:2311.01977*, 2023. 3
- [15] Jonathan Ho, Ajay Jain, and Pieter Abbeel. Denoising diffusion probabilistic models. *Advances in neural information processing systems*, 33:6840–6851, 2020. 2
- [16] Jonathan Ho, Tim Salimans, Alexey Gritsenko, William Chan, Mohammad Norouzi, and David J Fleet. Video diffusion models. *Advances in Neural Information Processing Systems*, 35:8633–8646, 2022. 2
- [17] Edward J Hu, Yelong Shen, Phillip Wallis, Zeyuan Allen-Zhu, Yuanzhi Li, Shean Wang, Lu Wang, and Weizhu Chen. Lora: Low-rank adaptation of large language models. *arXiv preprint arXiv:2106.09685*, 2021. 4
- [18] Pu Hua, Minghuan Liu, Annabella Macaluso, Yunfeng Lin, Weinan Zhang, Huazhe Xu, and Lirui Wang. Gensim2: Scaling robot data generation with multi-modal and reasoning llms. *arXiv preprint arXiv:2410.03645*, 2024. 3
- [19] Tao Huang, Guangqi Jiang, Yanjie Ze, and Huazhe Xu. Diffusion reward: Learning rewards via conditional video diffusion. In *European Conference on Computer Vision*, pages 478–495. Springer, 2025. 3
- [20] Eric Jang, Alex Irpan, Mohi Khansari, Daniel Kappler, Frederik Ebert, Corey Lynch, Sergey Levine, and Chelsea Finn. Bc-z: Zero-shot task generalization with robotic imitation learning. In *Conference on Robot Learning*, pages 991–1002. PMLR, 2022. 3
- [21] Xiaogang Jia, Qian Wang, Atalay Donat, Bowen Xing, Ge Li, Hongyi Zhou, Onur Celik, Denis Blessing, Rudolf Lioutikov, and Gerhard Neumann. Mail: Improving imitation learning with selective state space models. 2024. 3
- [22] Yunfan Jiang, Agrim Gupta, Zichen Zhang, Guanzhi Wang, Yongqiang Dou, Yanjun Chen, Li Fei-Fei, Anima Anandkumar, Yuke Zhu, and Linxi Fan. Vima: General robot manipulation with multimodal prompts. *arXiv preprint arXiv:2210.03094*, 2(3):6, 2022. 3
- [23] Pushkal Katara, Zhou Xian, and Katerina Fragkiadaki. Gen2sim: Scaling up robot learning in simulation with generative models. In *2024 IEEE International Conference on Robotics and Automation (ICRA)*, pages 6672–6679. IEEE, 2024. 3

- [24] Tsung-Wei Ke, Nikolaos Gkanatsios, and Katerina Fragkiadaki. 3d diffuser actor: Policy diffusion with 3d scene representations. *arXiv preprint arXiv:2402.10885*, 2024. 3
- [25] Alexander Khazatsky, Karl Pertsch, Suraj Nair, Ashwin Balakrishna, Sudeep Dasari, Siddharth Karamcheti, Soroush Nasiriany, Mohan Kumar Srirama, Lawrence Yunliang Chen, Kirsty Ellis, et al. Droid: A large-scale in-the-wild robot manipulation dataset. *arXiv preprint arXiv:2403.12945*, 2024. 4
- [26] Moo Jin Kim, Karl Pertsch, Siddharth Karamcheti, Ted Xiao, Ashwin Balakrishna, Suraj Nair, Rafael Rafailov, Ethan Foster, Grace Lam, Pannag Sanketi, et al. Openvla: An open-source vision-language-action model. *8th Annual Conference on Robot Learning*, 2024. 2, 3, 5, 6, 7
- [27] Woosuk Kwon, Zhuohan Li, Siyuan Zhuang, Ying Sheng, Lianmin Zheng, Cody Hao Yu, Joseph E. Gonzalez, Hao Zhang, and Ion Stoica. Efficient memory management for large language model serving with pagedattention. In *Proceedings of the ACM SIGOPS 29th Symposium on Operating Systems Principles*, 2023. 4
- [28] Tianhong Li, Yonglong Tian, He Li, Mingyang Deng, and Kaiming He. Autoregressive image generation without vector quantization. *arXiv preprint arXiv:2406.11838*, 2024. 3
- [29] Jacky Liang, Wenlong Huang, Fei Xia, Peng Xu, Karol Hausman, Brian Ichter, Pete Florence, and Andy Zeng. Code as policies: Language model programs for embodied control. In *2023 IEEE International Conference on Robotics and Automation (ICRA)*, pages 9493–9500. IEEE, 2023. 3
- [30] Fanqi Lin, Yingdong Hu, Pingyue Sheng, Chuan Wen, Jiacheng You, and Yang Gao. Data scaling laws in imitation learning for robotic manipulation, 2024. 3, 4
- [31] Pan Lu, Baolin Peng, Hao Cheng, Michel Galley, Kai-Wei Chang, Ying Nian Wu, Song-Chun Zhu, and Jianfeng Gao. Chameleon: Plug-and-play compositional reasoning with large language models. *Advances in Neural Information Processing Systems*, 36, 2024. 3
- [32] Jianlan Luo, Zheyuan Hu, Charles Xu, You Liang Tan, Jacob Berg, Archit Sharma, Stefan Schaal, Chelsea Finn, Abhishek Gupta, and Sergey Levine. Serl: A software suite for sample-efficient robotic reinforcement learning. *arXiv preprint arXiv:2401.16013*, 2024. 3
- [33] Yiyang Ma, Xingchao Liu, Xiaokang Chen, Wen Liu, Chengyue Wu, Zhiyu Wu, Zizheng Pan, Zhenda Xie, Haowei Zhang, Liang Zhao, et al. Janusflow: Harmonizing autoregression and rectified flow for unified multimodal understanding and generation. *arXiv preprint arXiv:2411.07975*, 2024. 3
- [34] Octo Model Team, Dibya Ghosh, Homer Walke, Karl Pertsch, Kevin Black, Oier Mees, Sudeep Dasari, Joey Hejna, Charles Xu, Jianlan Luo, Tobias Kreiman, You Liang Tan, Lawrence Yunliang Chen, Pannag Sanketi, Quan Vuong, Ted Xiao, Dorsa Sadigh, Chelsea Finn, and Sergey Levine. Octo: An open-source generalist robot policy. In *Proceedings of Robotics: Science and Systems*, Delft, Netherlands, 2024. 3, 5, 6
- [35] Abby O’Neill, Abdul Rehman, Abhinav Gupta, Abhiram Maddukuri, Abhishek Gupta, Abhishek Padalkar, Abraham Lee, Acorn Pooley, Agrim Gupta, Ajay Mandlekar, et al. Open x-embodiment: Robotic learning datasets and rt-x models. *arXiv preprint arXiv:2310.08864*, 2023. 4, 5
- [36] William Peebles and Saining Xie. Scalable diffusion models with transformers. In *Proceedings of the IEEE/CVF International Conference on Computer Vision*, pages 4195–4205, 2023. 2
- [37] Ethan Perez, Florian Strub, Harm De Vries, Vincent Dumoulin, and Aaron Courville. Film: Visual reasoning with a general conditioning layer. In *Proceedings of the AAAI conference on artificial intelligence*, 2018. 4
- [38] Dustin Podell, Zion English, Kyle Lacey, Andreas Blattmann, Tim Dockhorn, Jonas Müller, Joe Penna, and Robin Rombach. Sdxl: Improving latent diffusion models for high-resolution image synthesis. *arXiv preprint arXiv:2307.01952*, 2023. 2
- [39] Aaditya Prasad, Kevin Lin, Jimmy Wu, Linqi Zhou, and Jeannette Bohg. Consistency policy: Accelerated visuomotor policies via consistency distillation. *arXiv preprint arXiv:2405.07503*, 2024. 3
- [40] Krishan Rana, Jesse Haviland, Sourav Garg, Jad Abou-Chakra, Ian D Reid, and Niko Suenderhauf. Sayplan: Grounding large language models using 3d scene graphs for scalable task planning. *CoRR*, 2023. 3
- [41] Allen Z Ren, Justin Lidard, Lars L Ankile, Anthony Simeonov, Pulkit Agrawal, Anirudha Majumdar, Benjamin Burchfiel, Hongkai Dai, and Max Simchowitz. Diffusion policy policy optimization. *arXiv preprint arXiv:2409.00588*, 2024. 3
- [42] Moritz Reuss, Ömer Erdiñç Yağmurlu, Fabian Wenzel, and Rudolf Lioutikov. Multimodal diffusion transformer: Learning versatile behavior from multimodal goals. 2024. 3
- [43] Robin Rombach, Andreas Blattmann, Dominik Lorenz, Patrick Esser, and Björn Ommer. High-resolution image synthesis with latent diffusion models. In *Proceedings of the IEEE/CVF conference on computer vision and pattern recognition*, pages 10684–10695, 2022. 2
- [44] Lucy Xiaoyang Shi, Zheyuan Hu, Tony Z Zhao, Archit Sharma, Karl Pertsch, Jianlan Luo, Sergey Levine, and Chelsea Finn. Yell at your robot: Improving on-the-fly from language corrections. *arXiv preprint arXiv:2403.12910*, 2024. 4, 3
- [45] Laura Smith, Ilya Kostrikov, and Sergey Levine. A walk in the park: Learning to walk in 20 minutes with model-free reinforcement learning. *arXiv preprint arXiv:2208.07860*, 2022. 3
- [46] Peize Sun, Yi Jiang, Shoufa Chen, Shilong Zhang, Bingyue Peng, Ping Luo, and Zehuan Yuan. Autoregressive model beats diffusion: Llama for scalable image generation. *arXiv preprint arXiv:2406.06525*, 2024. 3
- [47] Chameleon Team. Chameleon: Mixed-modal early-fusion foundation models. *arXiv preprint arXiv:2405.09818*, 2024. 2
- [48] Hugo Touvron, Thibaut Lavril, Gautier Izacard, Xavier Martinet, Marie-Anne Lachaux, Timothée Lacroix, Baptiste Rozière, Naman Goyal, Eric Hambro, Faisal Azhar, et al. Llama: Open and efficient foundation language models. *arXiv preprint arXiv:2302.13971*, 2023.

- [49] Hugo Touvron, Louis Martin, Kevin Stone, Peter Albert, Amjad Almahairi, Yasmine Babaei, Nikolay Bashlykov, Soumya Batra, Prajwal Bhargava, Shruti Bhosale, et al. Llama 2: Open foundation and fine-tuned chat models. *arXiv preprint arXiv:2307.09288*, 2023. 2
- [50] Masatoshi Uehara, Yulai Zhao, Kevin Black, Ehsan Hajiramezani, Gabriele Scalia, Nathaniel Lee Diamant, Alex M Tseng, Tommaso Biancalani, and Sergey Levine. Fine-tuning of continuous-time diffusion models as entropy-regularized control. *arXiv preprint arXiv:2402.15194*, 2024. 3
- [51] Masatoshi Uehara, Yulai Zhao, Kevin Black, Ehsan Hajiramezani, Gabriele Scalia, Nathaniel Lee Diamant, Alex M Tseng, Sergey Levine, and Tommaso Biancalani. Feedback efficient online fine-tuning of diffusion models. *arXiv preprint arXiv:2402.16359*, 2024. 3
- [52] Dian Wang, Stephen Hart, David Surovik, Tarik Kelestemur, Haojie Huang, Haibo Zhao, Mark Yeatman, Jiuguang Wang, Robin Walters, and Robert Platt. Equivariant diffusion policy. *arXiv preprint arXiv:2407.01812*, 2024. 3
- [53] Peng Wang, Shuai Bai, Sinan Tan, Shijie Wang, Zhihao Fan, Jinze Bai, Keqin Chen, Xuejing Liu, Jialin Wang, Wenbin Ge, et al. Qwen2-vl: Enhancing vision-language model’s perception of the world at any resolution. *arXiv preprint arXiv:2409.12191*, 2024. 3
- [54] Xinlong Wang, Xiaosong Zhang, Zhengxiong Luo, Quan Sun, Yufeng Cui, Jinsheng Wang, Fan Zhang, Yueze Wang, Zhen Li, Qiying Yu, et al. Emu3: Next-token prediction is all you need. *arXiv preprint arXiv:2409.18869*, 2024. 3
- [55] Yixiao Wang, Yifei Zhang, Mingxiao Huo, Ran Tian, Xiang Zhang, Yichen Xie, Chenfeng Xu, Pengliang Ji, Wei Zhan, Mingyu Ding, et al. Sparse diffusion policy: A sparse, reusable, and flexible policy for robot learning. *arXiv preprint arXiv:2407.01531*, 2024. 3
- [56] Zhendong Wang, Zhaoshuo Li, Ajay Mandlekar, Zhenjia Xu, Jiaojiao Fan, Yashraj Narang, Linxi Fan, Yuke Zhu, Yogesh Balaji, Mingyuan Zhou, et al. One-step diffusion policy: Fast visuomotor policies via diffusion distillation. *arXiv preprint arXiv:2410.21257*, 2024. 3
- [57] Junjie Wen, Yichen Zhu, Jinming Li, Minjie Zhu, Kun Wu, Zhiyuan Xu, Ran Cheng, Chaomin Shen, Yaxin Peng, Feifei Feng, et al. Tinyvla: Towards fast, data-efficient vision-language-action models for robotic manipulation. *arXiv preprint arXiv:2409.12514*, 2024. 3, 5, 6
- [58] Junjie Wen, Yichen Zhu, Minjie Zhu, Jinming Li, Zhiyuan Xu, Zhengping Che, Chaomin Shen, Yaxin Peng, Dong Liu, Feifei Feng, and Jian Tang. Object-centric instruction augmentation for robotic manipulation. In *2024 IEEE International Conference on Robotics and Automation (ICRA)*, pages 4318–4325, 2024. 3
- [59] Chengyue Wu, Xiaokang Chen, Zhiyu Wu, Yiyang Ma, Xingchao Liu, Zizheng Pan, Wen Liu, Zhenda Xie, Xingkai Yu, Chong Ruan, et al. Janus: Decoupling visual encoding for unified multimodal understanding and generation. *arXiv preprint arXiv:2410.13848*, 2024. 3
- [60] Yecheng Wu, Zhuoyang Zhang, Junyu Chen, Haotian Tang, Dacheng Li, Yunhao Fang, Ligeng Zhu, Enze Xie, Hongxu Yin, Li Yi, et al. Vila-u: a unified foundation model integrating visual understanding and generation. *arXiv preprint arXiv:2409.04429*, 2024. 3
- [61] Jinheng Xie, Weijia Mao, Zechen Bai, David Junhao Zhang, Weihao Wang, Kevin Qinghong Lin, Yuchao Gu, Zhijie Chen, Zhenheng Yang, and Mike Zheng Shou. Show-o: One single transformer to unify multimodal understanding and generation. *arXiv preprint arXiv:2408.12528*, 2024. 3
- [62] Ge Yan, Yueh-Hua Wu, and Xiaolong Wang. Dnact: Diffusion guided multi-task 3d policy learning. *arXiv preprint arXiv:2403.04115*, 2024. 3
- [63] Zhecheng Yuan, Tianming Wei, Shuiqi Cheng, Gu Zhang, Yuanpei Chen, and Huazhe Xu. Learning to manipulate anywhere: A visual generalizable framework for reinforcement learning. *arXiv preprint arXiv:2407.15815*, 2024. 3
- [64] Michał Zawalski, William Chen, Karl Pertsch, Oier Mees, Chelsea Finn, and Sergey Levine. Robotic control via embodied chain-of-thought reasoning. *arXiv preprint arXiv:2407.08693*, 2024. 3, 4
- [65] Yanjie Ze, Nicklas Hansen, Yinbo Chen, Mohit Jain, and Xiaolong Wang. Visual reinforcement learning with self-supervised 3d representations. *IEEE Robotics and Automation Letters*, 8(5):2890–2897, 2023. 3
- [66] Yanjie Ze, Zixuan Chen, Wenhao Wang, Tianyi Chen, Xialin He, Ying Yuan, Xue Bin Peng, and Jiajun Wu. Generalizable humanoid manipulation with improved 3d diffusion policies. *arXiv preprint arXiv:2410.10803*, 2024. 3
- [67] Yanjie Ze, Yuyao Liu, Ruizhe Shi, Jiabin Qin, Zhecheng Yuan, Jiashun Wang, and Huazhe Xu. H-index: Visual reinforcement learning with hand-informed representations for dexterous manipulation. *Advances in Neural Information Processing Systems*, 36, 2024. 3
- [68] Yanjie Ze, Gu Zhang, Kangning Zhang, Chenyuan Hu, Muhao Wang, and Huazhe Xu. 3d diffusion policy: Generalizable visuomotor policy learning via simple 3d representations. In *ICRA 2024 Workshop on 3D Visual Representations for Robot Manipulation*, 2024. 3
- [69] Xiaohua Zhai, Basil Mustafa, Alexander Kolesnikov, and Lucas Beyer. Sigmoid loss for language image pre-training. In *Proceedings of the IEEE/CVF International Conference on Computer Vision*, pages 11975–11986, 2023. 3
- [70] Chuyang Zhao, Yuxing Song, Wenhao Wang, Haocheng Feng, Errui Ding, Yifan Sun, Xinyan Xiao, and Jingdong Wang. Monoformer: One transformer for both diffusion and autoregression. *arXiv preprint arXiv:2409.16280*, 2024. 3
- [71] Tony Z Zhao, Jonathan Tompson, Danny Driess, Pete Florence, Seyed Kamyar Seyed Ghasemipour, Chelsea Finn, and Ayzaan Wahid. Aloha unleashed: A simple recipe for robot dexterity. In *8th Annual Conference on Robot Learning*. 3
- [72] Chunting Zhou, Lili Yu, Arun Babu, Kushal Tirumala, Michihiro Yasunaga, Leonid Shamis, Jacob Kahn, Xuezhe Ma, Luke Zettlemoyer, and Omer Levy. Transfusion: Predict the next token and diffuse images with one multi-modal model. *arXiv preprint arXiv:2408.11039*, 2024. 3
- [73] Minjie Zhu, Yichen Zhu, Jinming Li, Junjie Wen, Zhiyuan Xu, Zhengping Che, Chaomin Shen, Yaxin Peng, Dong Liu,

Feifei Feng, and Jian Tang. Language-conditioned robotic manipulation with fast and slow thinking. In *2024 IEEE International Conference on Robotics and Automation (ICRA)*, pages 4333–4339, 2024. [3](#)

- [74] Minjie Zhu, Yichen Zhu, Jinming Li, Junjie Wen, Zhiyuan Xu, Ning Liu, Ran Cheng, Chaomin Shen, Yaxin Peng, Feifei Feng, et al. Scaling diffusion policy in transformer to 1 billion parameters for robotic manipulation. *arXiv preprint arXiv:2409.14411*, 2024. [3](#), [6](#)
- [75] Yichen Zhu, Zhicai Ou, Xiaofeng Mou, and Jian Tang. Retrieval-augmented embodied agents. In *Proceedings of the IEEE/CVF Conference on Computer Vision and Pattern Recognition*, pages 17985–17995, 2024. [3](#)

Diffusion-VLA:

Scaling Robot Foundation Models via Unified Diffusion and Autoregression

Supplementary Material

Table 4. Summarization for the number of demonstrations and average trajectory length for our real-world tasks.

#	Task	# of Demonstrations	Avg. Trajectory Length
1	Object selection	160	91
2	Flip the vertically placed pot	120	137
3	Place cube inside box with closed lid	50	146
4	Place cup onto the plate	100	107
5	Place cube into yellow/blue Box	100	90

6. Evaluation Tasks and Detailed Results

6.1. Evaluation Tasks

As described in Section 4, we evaluate our DiVLA and baselines on multi-task learning, factory sorting, zero-shot bin-picking, and table bussing. In this section, we provide details on these tasks. All of these tasks are depicted in Figure 10 and 11.

For multi-task learning, we evaluate all methods on 5 tasks for multi-task learning and 5 visual generalization tasks. We evaluate each method with a total of 77 trials for multi-task learning and 45 trials for visual generalization. We provide the number of demonstrations and the average length of these tasks in 4. A brief description of these tasks is as follows:

- **Object selection.** In this task, we evaluate the model’s ability to comprehend and act on user intent effectively. To do so, we design three distinct instructions, each requiring the robot to identify and pick up the appropriate object based on the user’s expressed intent. These instructions are intentionally diverse to test the model’s versatility and robustness in understanding varying contexts and nuances of user commands.
- **Flip the vertically placed pot.** In this task, we evaluate the model’s commonsense reasoning abilities. Specifically, the model must determine whether a vertically placed pot is oriented to the right or left and accurately identify its direction to position it correctly. This test assesses the model’s capacity to understand spatial orientation and apply logical reasoning to achieve the desired outcome.
- **Place cube inside box with closed lid.** In this task, we evaluate the model’s ability to reason about and execute a multi-step operation that involves manipulating objects with physical constraints. The robot must first identify the box with the closed lid, open the lid, and then place the cube inside the box. This task assesses the model’s planning, understanding of spatial relationships, and abil-

ity to perform actions in a sequence to achieve a desired goal.

- **Place cup onto the plate.** In this task, we test the model’s ability to perceive and reason about the spatial arrangement of objects in a structured environment. A plate is placed on a two-tiered shelf, and the robot must first identify which tier the plate is located on. And the robot needs to carefully place the cup onto the plate without disturbing the surrounding setup. This task evaluates the model’s spatial reasoning and precision in action.
- **Place cube into yellow/blue Box.** In this task, we assess the model’s ability to follow instructions and demonstrate spatial reasoning. The robot is presented with an instruction specifying a designated box, either yellow or blue, and is required to accurately identify the correct box based on the given instruction. Once identified, the robot must then place a cube inside the chosen box. This task tests not only the model’s comprehension of language-based directives but also its ability to integrate spatial awareness and execute precise actions.

Setup for visual generalization. In this setting, we assess the model’s robustness and ability to generalize its visual perception to different environmental conditions. The robot is required to perform manipulation tasks under challenging visual variations, including randomly placed distractors, distracting lighting conditions, and a colorful background. These variations test the model’s capacity to maintain focus on the primary task while filtering out irrelevant visual noise and adapting to dynamic visual environments. The goal is to ensure the robot can accurately identify and interact with objects despite significant deviations from standard settings.

Moreover, detailed descriptions for factory sorting, zero-shot bin-picking, and table bussing are provided in Sections 4.3, 4.4, and 4.5, respectively.

6.2. Detailed Results

In this section, we present the complete evaluation results for both the Franka and Bimanual AgileX robots, as detailed in Table 5. DiVLA-2B consistently demonstrates superior performance across the majority of tasks. Additionally, our findings highlight DiVLA-2B’s robust visual generalization capabilities, effectively adapting to changes in the surrounding environment.

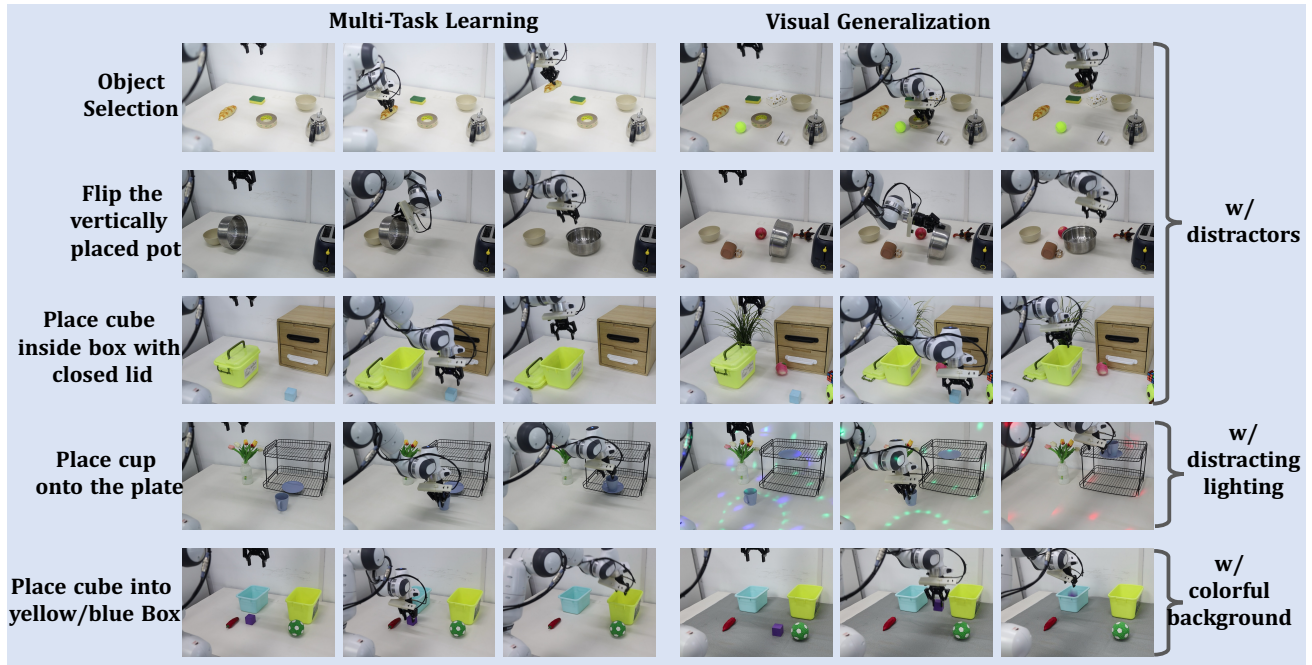


Figure 10. **Multi-task Learning and Visual Generalization.** We evaluate each method on multi-task learning and visual generalizations, including adding additional distractors, changing the background, and implementing colorful lighting. Each set of three images represents the initial state, intermediate state, and final state of one trial.

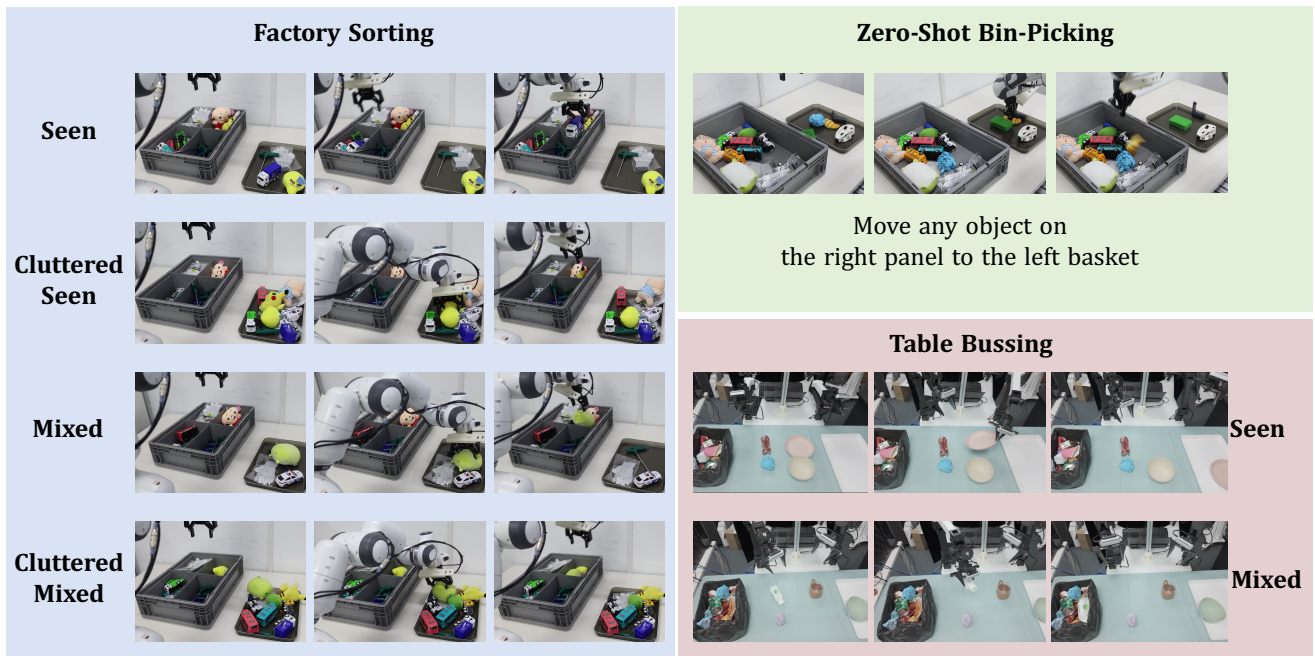


Figure 11. **Factory Sorting, Zero-Shot Bin-Picking and Table Bussing.** We further evaluate all robot policies on additional challenging tasks, including factory sorting, zero-shot bin-picking, and bimanual table bussing. These tasks involve previously unseen objects with diverse textures, varying heights, and different degrees of deformability (as illustrated in Figure 7 and Figure 8). Each set of three images represents the progression of a single trial, showcasing the initial state, intermediate state, and final state.

Table 5. **Detailed Experimental Results on both Franka and AgileX Aloha.**

Type	Task	Trails	DP	TinyVLA	Octo	OpenVLA	DiVLA-2B
Multi-Task Learning	Object Selection	33	22	23	19	24	33
	Flip the Vertically Placed Pot.	11	4	5	3	2	11
	Place Cube into Yellow/Blue Box	11	0	3	3	6	10
	Place Cup onto Plate	11	4	5	1	4	7
	Place Cube inside Box with Closed Lip	11	0	4	2	2	7
Visual Generalization	Object Selection	9	1	4	4	5	4
	Flip the Vertically Placed Pot.	9	1	4	1	1	6
	Place Cube into Yellow/Blue Box	9	0	2	0	3	6
	Place Cup onto Plate	9	2	2	0	3	6
	Place Cube inside Box with Closed Lip	9	0	1	2	0	4
More Challenging Tasks	Factory Sorting (Seen)	80	27	39	33	45	61
	Factory Sorting (Mixed)	80	11	25	27	36	50
	Factory Sorting (Cluttered Seen)	65	16	21	17	30	43
	Factory Sorting (Cluttered Mixed)	65	6	14	15	22	40
	Zero-Shot Bin-Picking	102	10	24	4	29	65
	Table Bussing (Seen)	48	22	-	-	0	35
	Table Bussing (Mixed)	48	15	-	-	0	34

Table 6. **Inference speed for DiVLA.** We report the inference speed for DiVLA on A6000 GPU.

Method	DiVLA-2B	DiVLA-7B	OpenVLA-7B
Control Frequency	82Hz	42Hz	5Hz



Figure 12. **View Generalization.** We evaluate DP, OpenVLA, and DiVLA-2B in the view shifting setting, where we use completely different camera positions to capture images. The blue part indicates the original camera positions, while the red part indicates the new camera positions.

Table 7. **Experimental results for view shifting generalization.** We conduct view shifting generalization on factory sorting task. The experimental setup is shown in Figure 12. We report the success rate for each policy. Each method is evaluate with 5 trails.

Task \ Method	Diffusion Policy	OpenVLA	DiVLA-2B
Sorting	0	0	60

7. Implementation Details

For the baselines, we follow a uniform training strategy to ensure consistency. For OpenVLA, we follow the original implementation which only uses a single camera. We also test OpenVLA with three camera views, where each view goes through the same visual encoder and concatenates its outputs for further process. We observe some performance improvement over multiple camera views. For instance, for sorting task, the average success rate will increase from 32.3% to 45.3%. Nevertheless, since most of the existing works only report the OpenVLA baseline with a single camera view, we only report experimental results for this setting. More details can refer to TinyVLA [57]. OpenVLA’s pre-trained weights are used, and we fine-tune the model on our dataset with a learning rate of $2e-5$. For the Diffusion Policy, we employ DistilBERT to encode language instructions, adopting a methodology similar to YAY [44]. All models are trained for the same number of epochs, and only the final checkpoint is used for evaluation. To ensure a fair comparison, we avoid cherry-picking the checkpoint.

8. More Experiments

8.1. View Shifting Generalization

Imitation learning often struggles to generalize its capabilities to novel viewpoints. In this study, we evaluate the view generalization performance of DP, OpenVLA, and DiVLA-2B in a factory sorting task. The experimental setup is illustrated in Figure 12. As shown in Table 7, OpenVLA exhibits poor generalization to view shifts. In contrast, DiVLA-2B demonstrates notable robustness in view gen-

eralization, achieving a success rate of 60%. This result highlights the advantages of leveraging pretraining on large-scale robotic datasets to enhance generalization capabilities.

8.2. Efficient Inference

Fast inference speed is critical for deploying VLA models in real-world applications. However, as models grow in size and complexity, their inference speed tends to decrease significantly on server-grade hardware. To address this challenge and enhance model performance, we deploy our models on the vLLM framework [27]. This approach leverages optimized infrastructure to maximize inference efficiency. In Table 6, we present a comparative analysis of control frequencies for DiVLA-2B, DiVLA-7B, and OpenVLA (a 7B model). Our results demonstrate remarkable speed improvements: the DiVLA-2B model achieves an impressive 82 Hz on an A6000 GPU, showcasing exceptional performance. Similarly, DiVLA-7B achieves a control frequency of 42 Hz, which is 8 times faster than OpenVLA at the same model size. These findings underscore the effectiveness of our optimizations in maintaining scalability without sacrificing speed, paving the way for broader real-world applicability of VLA models.

Notably, we avoid using action chunking techniques employed in other works, such as Data-Scaling-Laws [30] and π_0 [7], as we find that while action chunking can improve inference speed, it adversely impacts generalization performance. Another key observation is that our model experiences significant performance degradation when evaluated at lower bit precisions, such as 8-bit and 4-bit. This aligns with findings in OpenVLA, which highlight performance fluctuations introduced by quantization. These results suggest that current VLA models may require specifically designed quantization methods to maintain performance while achieving fast inference speeds at low precision.

8.3. Model Scaling

An important consideration for pure end-to-end neural networks is assessing their ability to scale effectively. As the model size and data volume grow, the performance of the model should ideally improve. To evaluate this scalability, we conducted additional experiments on two challenging tasks: factory sorting and zero-shot bin-picking. These tasks provide rigorous benchmarks to measure how increased model capacity and pre-training data influence performance. The detailed experimental results are presented in Table 8.

Our analysis highlights significant performance improvements when larger models and more extensive pre-training datasets are utilized. For example, the DiVLA-7B model demonstrates substantial gains over the DiVLA-2B model, achieving improvements of 8.7% and 3.0% in success rates for the factory sorting and bin-picking

Table 8. **Experimental results for model scaling.**

Tasks/Models	DiVLA-2B	DiVLA-7B	DiVLA-72B
Sorting	66.2	74.9	82.4
Bin Picking	63.7	66.7	75.9

Table 9. **VQA for DiVLA.** We test DiVLA’s ability to answer questions based on visual signals.

Question	Object/Scene	Answer	Correct
What is the object?		Toy Tiger	✗
		Tulip	✓
		Orange	✓
What is the object’s color?		Brown	✓
		Blue	✓
		Green	✓
Describe the scene.		The cube is on the right side of yellow pepper	✓
		The ball is on the top of a holder	✗

tasks, respectively. This underscores the benefits of scaling model size, which enables better representation learning and decision-making capabilities.

Moreover, scaling up to 72B parameters yields even greater performance boosts. These larger models not only achieve higher success rates in in-distribution scenarios but also exhibit superior generalization to out-of-distribution setups. This improvement reflects the models’ enhanced ability to handle variability in task environments, unseen object properties, and dynamic conditions.

8.4. DiVLA can do Visual-Question-Answering

Previous works, such as RT-2 [9] and ECoT [64], have suggested that co-training with vision-language data helps preserve basic conversational functionality for Vision-Language Action (VLA) data. In this section, we demonstrate that despite not being co-trained with vision-language data, our method retains its chatting capability and is proficient in performing common visual-question-answering (VQA) tasks. However, these works have neither provided concrete examples of chat interactions nor open-sourced their results, leaving it unclear to what extent conversational capabilities are retained in such models. We give a few examples in Table 9.

When prompted to identify objects, we observe that the model demonstrates the ability to recognize some items accurately, such as tulips and oranges. However, it struggles with more nuanced distinctions; for instance, DiVLA mis-

takenly identifies a toy dragon as a toy tiger, likely due to its reliance on color features rather than other distinguishing characteristics like shape or texture.

Interestingly, we observe that the model demonstrates strong sensitivity to color, consistently providing correct answers to all three questions focusing on an object’s color. This highlights a notable strength in color recognition but also reveals limitations in processing broader visual features for complex tasks. To further assess its capabilities, we tested the model with a simple scene description task, requiring it to describe spatial relationships between objects. The model successfully interpreted spatial relationships, such as identifying that one object is on the right or on top of another. However, it often failed to recognize objects correctly. For example, DiVLA misclassified a football as a regular ball.

Notably, these objects were not included in the model’s pre-training or fine-tuning data. However, the pre-trained VLM may have encountered similar objects during its pre-training phase, enabling it to recognize them correctly in some cases. This observation underscores the importance of leveraging pre-trained VLMs as a foundation for end-to-end visuomotor learning, as they provide a strong prior understanding of visual concepts that can significantly enhance downstream performance in complex tasks.